Brief report

STAT6 gain-of-function variant exacerbates multiple allergic symptoms

Ichiro Takeuchi, MD,[a,b]* Kumiko Yanagi, DDSc, PhD,[c]* Shuji Takada, PhD,[d] Toru Uchiyama, MD, PhD,[e] Arisa Igarashi, PhD,[c,f] Kenichiro Motomura, MD, PhD,[f] Yuka Hayashi, MD,[f] Naoko Nagano, MD,[f] Ryo Matsuoka, MD,[f] Hiroki Sugiyama, MD,[f] Takako Yoshioka, MD, PhD,[g] Hirohisa Saito, MD, PhD,[f] Toshinao Kawai, MD, PhD,[e] Yumiko Miyaji, MD, PhD,[h] Yusuke Inuzuka, MD,[h] Yoichi Matsubara, MD, PhD,[i] Yukihiro Ohya, MD, PhD,[h] Toshiaki Shimizu, MD, PhD,[b] Kenji Matsumoto, MD, PhD,[f] Katsuhiro Arai, MD, PhD,[a,h] Ichiro Nomura, MD, PhD,[h,j] Tadashi Kaname, MD, PhD,[c] and Hideaki Morita, MD, PhD[f,h] *Tokyo, Japan*

GRAPHICAL ABSTRACT

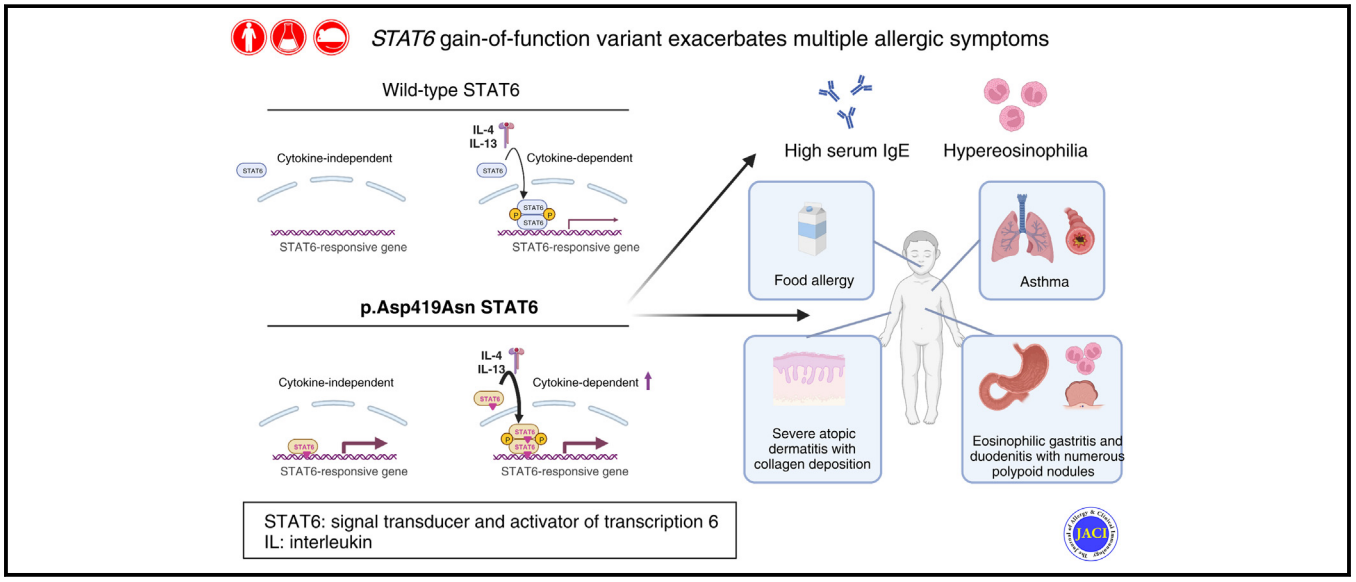

From [a]the Center for Pediatric Inflammatory Bowel Disease, Division of Gastroenterology, National Center for Child Health and Development, [b]the Department of Pediatrics and Adolescent Medicine, Juntendo University Graduate School of Medicine, Departments of [c]Genome Medicine and [d]Systems BioMedicine, National Research Institute for Child Health and Development, [e]the Division of Immunology, National Center for Child Health and Development, [f]the Department of Allergy and Clinical Immunology, National Research Institute for Child Health and Development, [g]the Department of Pathology and [h]the Allergy Center, National Center for Child Health and Development, [i]the National Research Institute for Child Health and Development and [j]the Division of Eosinophilic Gastrointestinal Disorders, National Research Institute for Child Health and Development, Tokyo.

*These 2 authors contributed equally to this study.

This study was supported in part by Initiative on Rare and Undiagnosed Diseases (grant nos. 19ek0109301s and 20ek0109301h) from the Japanese Agency for Medical Research and Development (AMED); National Grants-in-Aid to the National Center for Child Health and Development (grant nos. 2019A-3 [to K.A.], 2020B-10 [to I.T.], 2020B-2 [to K.M.], #29-2 [to H.M.], and 2022B-11 [to H.M.]); a Health, Labor and Welfare Sciences Research Grant for Research on Policy Planning and Evaluation for Rare and Intractable Diseases, from the Ministry of Health, Labor and Welfare (grant no. 20FC1016 [to I.N.]); and a Health, Labor and Welfare Sciences Research Grant (grant no. 21FE2001 [to H.M.]).

Data availability: The data sets generated and/or analyzed during the current study are available from the corresponding author on reasonable request.

Ethical considerations: This report was approved by the Institutional Review Board of the National Center for Child Health and Development, Tokyo, Japan (#378, #725, #926). Written informed consent from the patient's parents and assent from the patient were obtained when appropriate. All animal protocols were approved by the Animal Care and Use Committee of the National Research Institute for Child Health and Development, Tokyo, Japan (#A2017-006-C03). Recombinant DNA experiments were conducted in accordance with the approved protocol (#17-3).

Disclosure of potential conflict of interest: H. Morita has received a research grant from GlaxoSmithKline. The rest of the authors declare that they have no relevant conflicts of interest.

Received for publication July 5, 2022; revised November 29, 2022; accepted for publication December 5, 2022.

Corresponding author: Hideaki Morita, MD, PhD, or Tadashi Kaname, MD, PhD, or Ichiro Nomura, MD, PhD, National Research Institute for Child Health and Development, Tokyo, Okura 2-10-1, Setagaya Ward, Tokyo 157-8535, Japan. E-mail: morita-hi@ncchd.go.jp. Or: kaname-t@ncchd.go.jp. Or: nomura-i@ncchd.go.jp. Or: Katsuhiro Arai, MD, PhD, Center for Pediatric Inflammatory Bowel Disease, Division of Gastroenterology, National Center for Child Health and Development, Okura 2-10-1, Setagaya Ward, Tokyo, 157-8535, Japan. E-mail: arai-k@ncchd.go.jp.

0091-6749/$36.00

https://doi.org/10.1016/j.jaci.2022.12.802

Background: Allergic diseases were long considered to be complex multifactorial disorders. However, recent findings indicate that severe allergic inflammation can be caused by monogenic immune defects.
Objectives: We sought to clarify the molecular pathogenesis of a patient with early-onset multiple allergic diseases, a high serum IgE level, hypereosinophilia, treatment-resistant severe atopic dermatitis with increased dermal collagen fiber deposition, and eosinophilic gastrointestinal disorder with numerous polypoid nodules.
Methods: A missense variant in *STAT6* was identified, and its function was examined using peripheral blood, transfected HEK293 cells, lymphoblastoid cell lines, and knock-in mice with the corresponding mutation.
Results: Whole-exome sequencing identified a *de novo* heterozygous missense variant in signal transducer and activator of transcription 6 (*STAT6*) (p.Asp419Asn). Luciferase reporter assay revealed that the transcriptional activity of this STAT6 mutant was upregulated even without IL-4 stimulation. Phosphorylation of STAT6 was not observed in either the patient's T_H2 cells or lymphoblastoid cell lines without stimulation, whereas it was induced more strongly in both by IL-4 stimulation compared with healthy controls. STAT6 protein was present in the nuclear fraction of the lymphoblastoid cell lines of the patient even in the absence of IL-4 stimulation. The patient's gastric mucosa showed upregulation of STAT6-, fibrosis-, and germinal center formation–related molecules. Some of the knock-in mice with the corresponding mutation spontaneously developed dermatitis with skin thickening and eosinophil infiltration. Moreover, serum IgE levels and mRNA expression of type 2 cytokines were increased in the knock-in mice—with or without development of spontaneous dermatitis—compared with the wild-type mice.
Conclusions: A novel *STAT6* gain-of-function variant is a potential cause of primary atopic disorders. (J Allergy Clin Immunol 2023;■■■:■■■-■■■.)

Key words: *STAT6, hyper-IgE syndrome, hypereosinophilia, primary atopic disorders, atopic dermatitis, eosinophilic gastrointestinal disorder*

Abbreviations used
EGID: Eosinophilic gastrointestinal disorder
EoG: Eosinophilic gastritis
GOF: Gain-of-function
LCL: Lymphoblastoid cell line
PAD: Primary atopic disorder
STAT6: Signal transducer and activator of transcription 6
WT: Wild-type

INTRODUCTION

Type 2 inflammation, characterized by a high serum IgE level and hypereosinophilia, is one of the major hallmarks of allergic diseases, and it is mediated mainly by type 2 cytokines. Among them, IL-4 and IL-13 mediate a broad array of functions, including induction of T_H2 differentiation and IgE class-switching in B cells, via their downstream molecules, that is, signal transducer and activator of transcription 6 (STAT6).[1] Together with recent findings of genome-wide association studies,[2,3] it is known that IL-4/IL-13/STAT6 signaling plays a central role in allergic inflammation.

Allergic diseases have been thought to be complex multifactorial disorders caused by a combination of genetic and environmental factors.[2] However, recent advances in immunogenetics have revealed that severe allergic inflammation may be the sole or earliest manifestation of monogenic immune defects.[4-7] Based on these findings, the term "primary atopic disorders (PADs)" was recently coined to describe a group of heritable monogenic allergic diseases.[8] To date, variants of 39 genes—including *STAT3* and *DOCK8*, causes of hyper-IgE syndrome—have been identified as being associated with PADs.[4] However, there have been no reports of PAD-inducing variants of *STAT6*. Here, we report our identification of a *STAT6* gain-of-function (GOF) variant in a patient who exhibited early-onset multiple allergic diseases, a high serum IgE level, hypereosinophilia, severe atopic dermatitis with increased dermal collagen fiber deposition, and eosinophilic gastrointestinal disorders (EGIDs) with numerous polypoid nodules in the pylorus and duodenal bulb.

RESULTS AND DISCUSSION

The patient is a boy with no family history of allergic, inflammatory, or immunologic disorders. He developed persistent diarrhea immediately after birth and severe systemic eczema at age 3 weeks. His itchy eczema was refractory to conventional treatment with topical steroids. He also developed IgE-mediated food allergy to cow's milk at age 4 months and later became sensitized to various foods. He had several wheezing episodes from infancy, and asthma was diagnosed later on the basis of airway hyperresponsiveness. He exhibited short stature and failure to thrive from infancy (Fig 1). At age 2 years, he developed palpebral edema with hypoalbuminemia in addition to diarrhea and was diagnosed with EGIDs, that is, eosinophilic gastritis (EoG) and duodenitis (EoD),[9] based on the histological findings. His symptoms underwent repeated exacerbation and remission. At age 4 years, he developed abdominal pain and vomiting in addition to diarrhea. Gastrointestinal endoscopy found numerous polypoid nodules in the pylorus and duodenal bulb (Fig 2, *A* and *B*). Histological examination revealed significant eosinophilic infiltration (Fig 2, *C* and *D*). At the same time, his itchy eczema worsened, accompanied by thickening of his entire skin even though he was being treated with a highly potent topical corticosteroid (Fig 2, *E*). Histological examination of the skin showed epidermal hyperplasia and inflammatory cell infiltration with increased collagen fiber deposition in the dermal layer (Fig 2, *F*). These symptoms and endoscopic findings were improved by systemic corticosteroid treatment. However, the symptoms relapsed when the prednisolone dose was decreased. Because his serum IgE level was already extremely high (14,768 IU/mL) at age 9 months, PADs were suspected. The patient did not have specific features for hyper-IgE syndrome (hyper-IgE syndrome score: 16)[10,11] or other primary immunodeficiencies, but he had a high T_H2-cell proportion (Table I).

Trio-based whole-exome sequencing analysis revealed a heterozygous missense variant in *STAT6* (NM_003153:c.1255G>A (p.Asp419Asn)) that was not found in his healthy parents or brother, indicating that the variant was *de novo* (Fig 3, *A* and

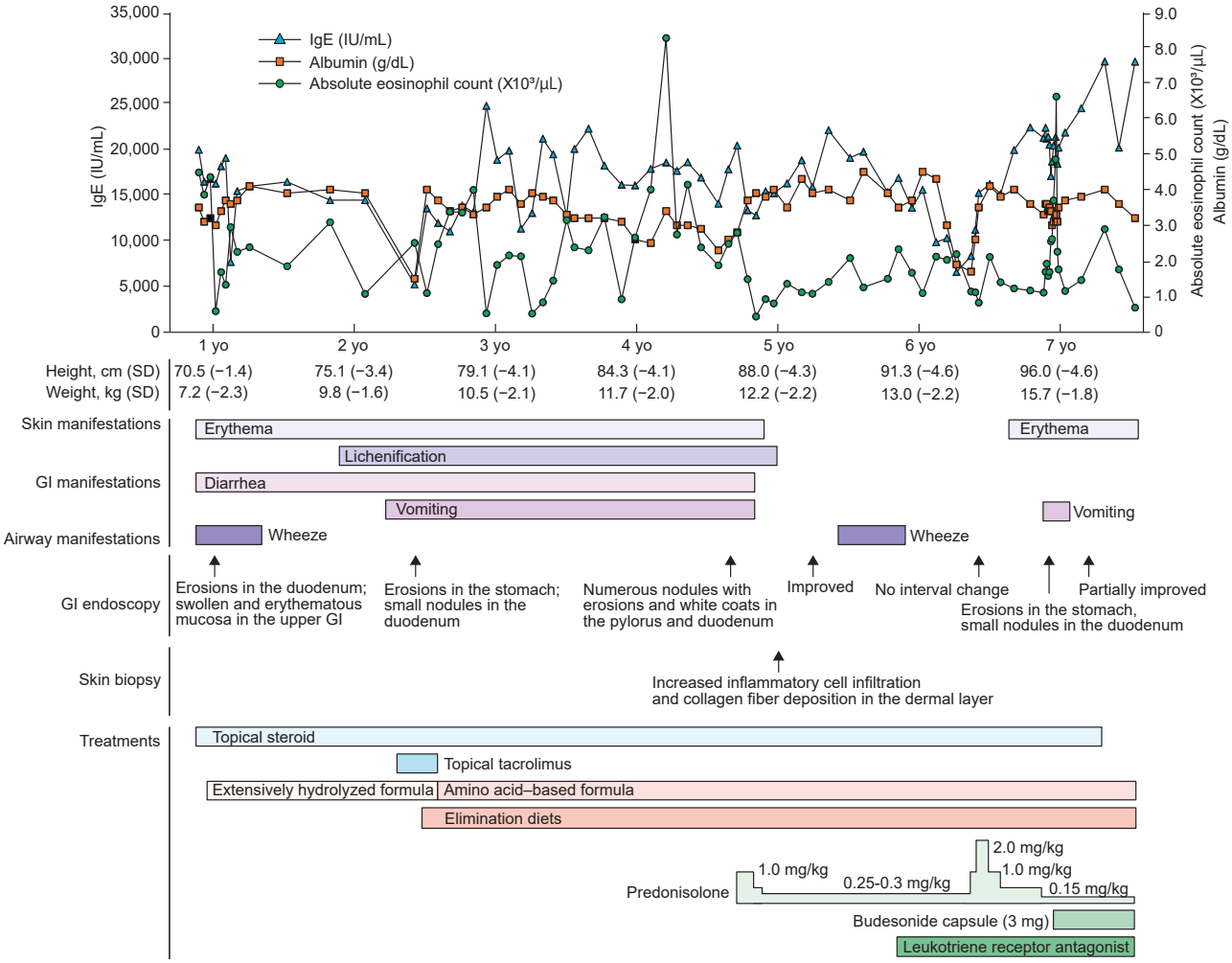

FIG 1. Demographic characteristics of the patient. The timeline describes the main clinical manifestations, body height and weight, laboratory tests, findings of endoscopy and skin biopsy, and treatments of the patient. The patient's characteristics were early-onset severe multiple allergic symptoms with a high serum IgE level, hypereosinophilia, large polypoid nodules in the stomach and duodenum, and collagen fiber deposition in the dermal layer. The timeline shows that the symptoms and findings varied with the presence/absence of systemic corticosteroid treatments. *GI*, Gastrointestinal; *yo*, year old.

B). Other genetically cosegregated pathogenic variants were not found among genes associated with severe allergies (see Table E1 in this article's Online Repository at www.jacionline.org). The variant was located close to the DNA-binding site of STAT6 (Fig 3, *C* and *D*). It is registered in dbSNP (rs11172102, http://www.nebi.nlm.gov/SNP), but not in the gnomAD database (https://gnomad.broadinstitute.org/), ToMMo (https://www.megabank.tohoku.ac.jp), or our in-house exome sequencing data.

To test the effects of this variant, constructs containing synthesized *STAT6* (STAT6 wild-type [WT]) or mutant *STAT6* (c.1255G>A; STAT6 mutant) were transfected into HEK293 cells.[13] Luciferase reporter assay using CCL26/eotaxin-3 promoter revealed that the transcriptional activity of this STAT6 mutant was upregulated even without IL-4 stimulation, whereas upregulation of the STAT6 WT was dependent on stimulation with IL-4 (Fig 3, *E*). These findings suggest that p.Asp419Asn STAT6 protein found in this patient is a GOF phenotype. Next, we used peripheral blood and lymphoblastoid cell lines (LCLs) to examine the effect of this *STAT6* variant on phosphorylation of STAT6 and its localization. There was no spontaneous STAT6 phosphorylation in peripheral blood T_H2 cells from either the patient or control, or in LCLs of the patient and his parents in the absence of IL-4 stimulation, whereas, on IL-4 stimulation, phosphorylation was induced in all (Fig 3, *F*, *G*, and *H*). Interestingly, STAT6 protein was present in the nuclear fraction of the LCLs of the patient even in the absence of IL-4 stimulation, but not in those of his parents (Fig 3, *G*). Moreover, phosphorylation of STAT6 was induced more strongly in the LCLs of the patient than in those of the parents on IL-4 stimulation (Fig 3, *G* and *H*). That induction was suppressed by Janus kinase inhibitors (Fig 3, *I*). These findings indicate that the p.Asp419Asn variant is involved in stronger phosphorylation of STAT6 protein and localization of STAT6 protein, even in the absence of IL-4 stimulation. Although the mechanisms of how p.Asp419Asn STAT6 protein is translocated into the nucleus in the absence of phosphorylation remain unclear, a similar phenomenon was observed in somatic variants of the p.Asp419 hotspot in STAT6 derived from follicular lymphomas.[14]

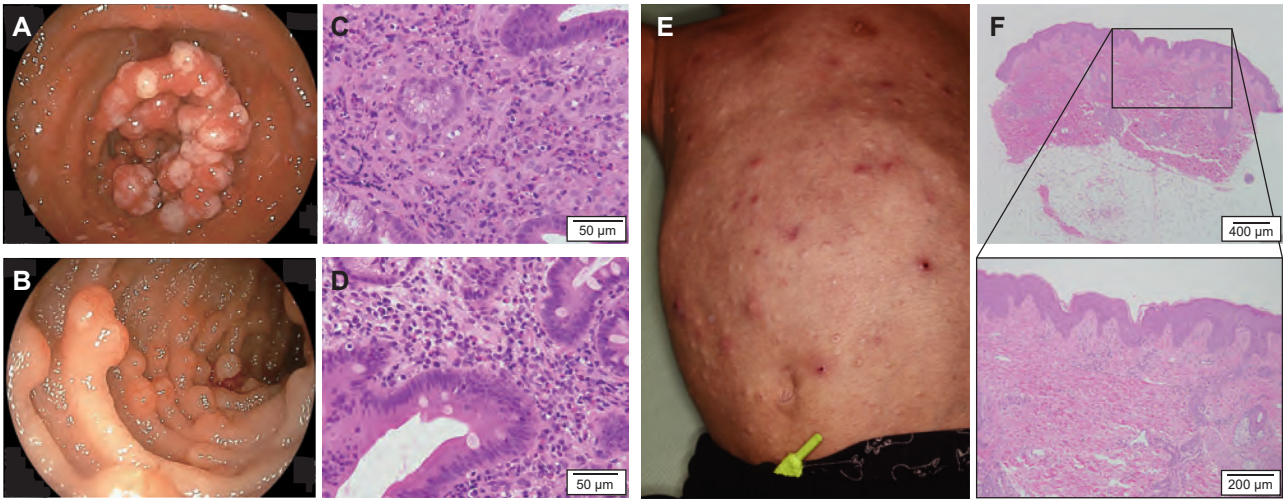

FIG 2. Features of the patient's skin and gastrointestinal tract. **A** and **B,** Endoscopic findings for the stomach and duodenum, respectively, at the age of 4 years. Diffuse polypoid nodules with swollen and erythematous mucosa are seen in the upper gastrointestinal tract. Numerous nodules with erosion and white coats are seen in the pylorus and duodenal bulb. **C** and **D,** Pathological findings for the gastric and duodenal mucosa, respectively, at the age of 4 years, showing significant eosinophil infiltration (>100/hpf in the pylorus; >25/hpf in the duodenum). **E,** Dermatologic findings of eczema with increased skin thickness and marked lichenification despite treatment with topical corticosteroids. **F,** Pathological findings for the affected skin. Increased inflammatory cell infiltration and collagen fiber deposition are seen in the dermal layer.

TABLE I. Immunologic characteristics of the patient with GOF STAT6 variant

	Age at evaluation					
	11 mo		2.8 y		4.6 y	
Immunologic profile	**Patient**	**Reference range**	**Patient**	**Reference range**	**Patient**	**Reference range**
Absolute lymphocyte count (cells/μL)	9,000	(2,800-4,800)*	5,100	(2,100-4,500)*	6,400	(2,000-2,900)*
Lymphocyte subsets						
$CD3^+$ T cells (/μL)	7,137	(1,300-3,700)*	3,810	(1,300-3,400)*	4,121	(1,400-2,400)*
$CD4^+$ T cells (/μL)	5,706	(1,800-3,600)*	2,279	(1,300-3,500)*	2,956	(1,400-2,100)*
$CD25^+$ $CD127^+$ regulatory T cells (/μL)	117	(120-170)*	50	(50-140)*	48	(60-80)*
$CD45RA^-$ $CXCR5^-$ $CRTH2^+$ cells (%)	NA		NA		21.3	(3.8-8.2)†
$CD45RA^-$ $CXCR5^-$ $CCR6^-$ $CXCR3^+$ cells (%)	NA		NA		15.0	(25.2-39.3)†
$CD45RA^-$ $CXCR5^-$ $CCR6^+$ $CXCR3^+$ cells (%)	NA		NA		4.9	(21.6-37.9)†
$CD45RA^-$ $CXCR5^-$ $CCR6^+$ $CXCR3^-$ cells (%)	NA		NA		14.3	(15.1-21.6)†
$CD3^-$ $CD4^+$ cells (/μL)	9	(6-8)*	15	(1-14)*	13	(<1)*
$CD8^+$ T cells (/μL)	2,619	(840-1,100)*	1,234	(630-1,300)*	1,945	(420-660)*
$CD16^+$ $CD56^+$ NK cells (/μL)	432	(180-990)*	153	(90-890)*	186	(110-120)*
$CD56^+$ $CD3^+$ NK T cells (/μL)	45	(10-30)*	26	(10-30)*	70	(20-50)*
$CD19^+$ B cells (/μL)	1,233	(430-880)*	1,046	(400-920)*	762	(410-440)*
CD38-high IgM- plasmablasts (/μL)	6	(210-240)*	9	(10-150)*	30	(40-130)*
$CD27^+$ IgM- class-switch recombination B cells (/μL)	43	(230-260)*	53	(30-180)*	47	(70-170)*
$CD38^+$ IgM-high transitional B cells (/μL)	18	(40-590)*	43	(60-530)*	28	(30-50)*
$CD27^+$ memory B cells (/μL)	171	(70-130)*	245	(70-150)*	186	(60-130)*
Absolute eosinophil count (cells/μL)	4,350	(<500)*	3,990	(<500)*	3,450	(<500)*
Immunoglobulin profile						
IgG level (mg/dL)	846	(380-1,020)‡	851	(500-1,280)‡	496	(560-1,390)‡
IgA level (mg/dL)	43	(10-59)‡	102	(20-149)‡	158	(31-202)‡
IgM level (mg/dL)	72	(58-209)‡	105	(60-270)‡	73	(66-288)‡
IgE level (IU/mL)	16,700	(NA)‡	13,100	(7-1,400)‡	17,107	(10-2,200)‡
TSLP (pg/mL)	4,557	(<1,367)‡	7,807	(<743)‡	4,198	(<743)‡

CD, Cluster of differentiation; *CXCR*, CXC chemokine receptor; *CCR*, CC chemokine receptor; *CRTH2*, chemoattractant receptor expressed on T_H2 cells; *NK*, natural killer; *Ig*, immunoglobulin; *TSLP*, thymus and activation-regulated chemokine.

*Reference ranges of lymphocyte subsets for the patient at each age were derived from age-matched patients with inflammatory bowel disease.

†These reference ranges were derived from healthy controls aged from 12 to 13 y.

‡These reference ranges are derived from reference intervals of clinical tests in Japanese children.[12]

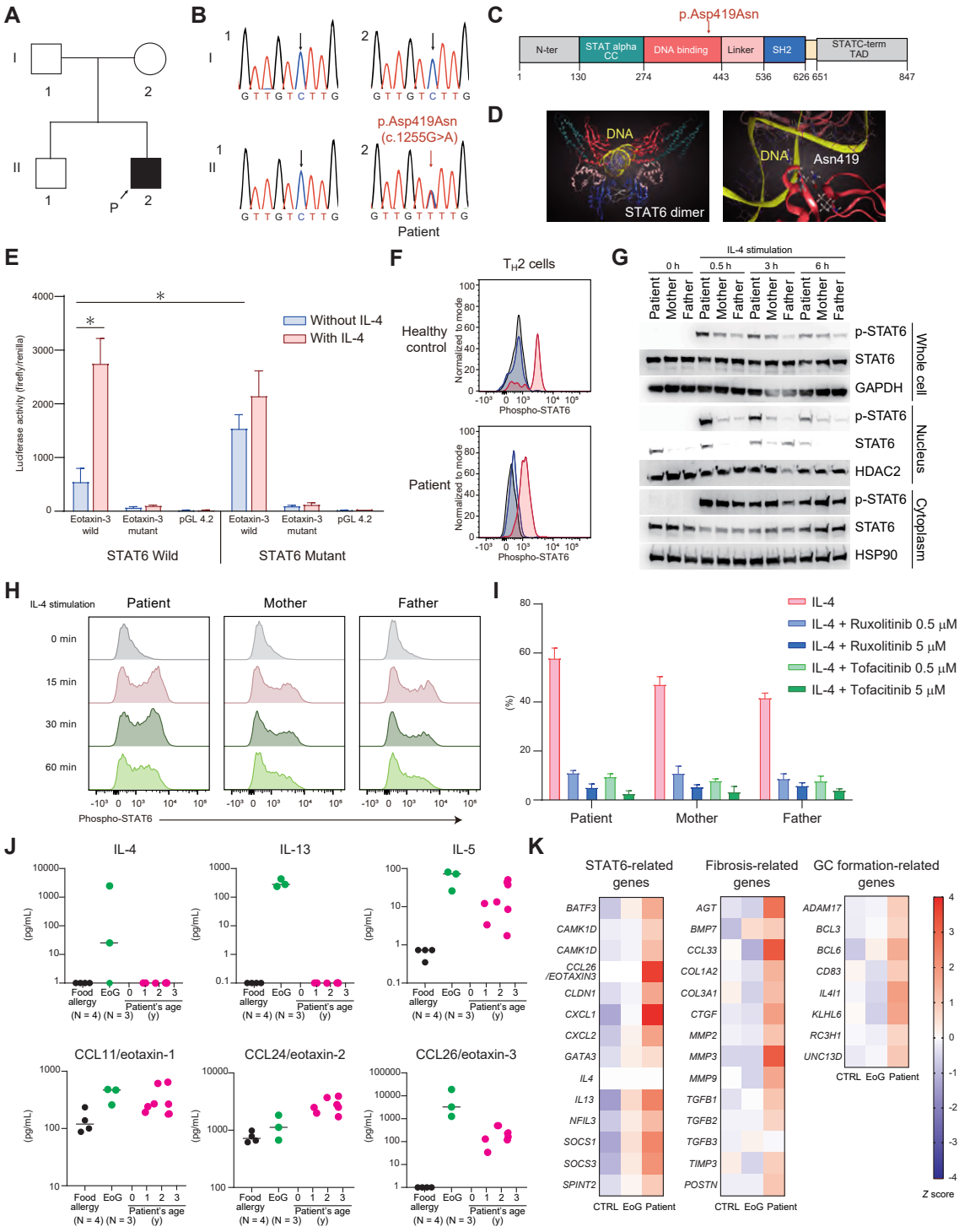

FIG 3. STAT6 variant in the patient and its function. **A,** Family pedigree. **B,** Genotypes by Sanger sequencing of genomic DNA samples. **C,** Schematic representation of the STAT6 protein. **D,** Structure of the mutant STAT6 dimer in a complex with double-stranded DNA (yellow). Each domain is shown in the same color as in Fig 3, *C*. **E,** Luciferase reporter assay using the eotaxin-3 promoter (mean + SD). **P* < .05. **F,** Phosphorylation of STAT6 in T_H2 cells. **G,** Western blot of STAT6 and p-STAT6 in LCLs. **H,** Time course of phosphorylation of STAT6 after IL-4 stimulation in LCLs. **I,** The effects of JAK inhibitors on IL-4–induced phosphorylation of STAT6 in LCLs. **J,** The serum cytokine levels of the patient with the *STAT6* variant (patient, n = 1; dots indicate the level at different time points), patients with IgE-mediated food allergy (food allergy, n = 4), and patients with EoG (n = 3). **K,** Gene expression profiles of gastric mucosa from the patient with the *STAT6* variant (patient, n = 1), control individuals (CTRL, n = 3; average expression level of 3 individuals), and patients with EoG (n = 3; average expression level of 3 individuals). *GC*, Germinal center.

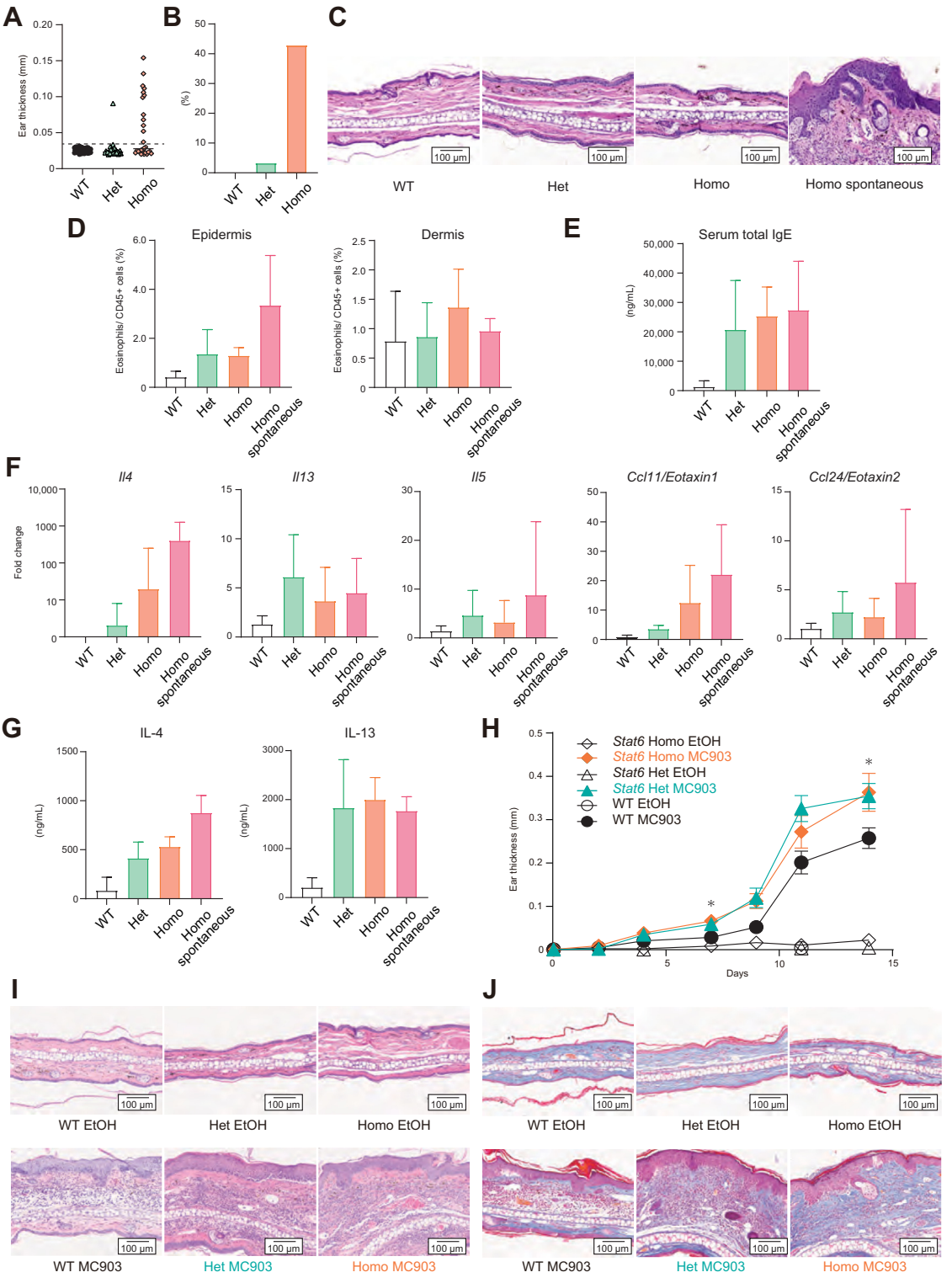

FIG 4. Phenotypes of mice with p.Asp419Asn *STAT6* variant. **A,** Ear thickness of the WT (n = 28) mice, knock-in mice carrying a heterozygous (*Stat6*$^{D419N/wt}$; Het, n = 30), and homozygous (*Stat6*$^{D419N/D419N}$; Homo, n = 28) mutation. The dashed line represents the +3SD, which determines spontaneous inflammation. **B,** Percentages of the mice that developed spontaneous dermatitis. **C,** Histological findings by hematoxylin-eosin staining. **D,** Percentage of eosinophils in skin (WT, n = 10; Het, n = 11; Homo, n = 4; Homo spontaneous, n = 3). **E,** Total IgE levels in sera (WT, n = 10; Het, n = 12; Homo, n = 3; Homo spontaneous, n = 4). **F,** mRNA expressions in skin (WT, n = 9; Het, n = 9; Homo, n = 10; Homo spontaneous, n = 5). **G,** IL-4 and IL-13 levels in the culture supernatant of cervical lymph node cells stimulated with phorbol 12-myristate 13-acetate/ionomycin (WT, n = 4; Het, n = 6; Homo, n = 2; Homo spontaneous, n = 3). **H,** Ear thickness (mean + SEM). The Kruskal-Wallis test was used to analyze differences among MC903-treated WT, Het, and Homo. **P* < .05. **I,** Histological findings by hematoxylin-eosin staining. **J,** Histological findings by Masson's trichrome staining.

To better understand the pathophysiology of the patient's condition, we analyzed the serum cytokine/chemokine levels and the gene expression profile of the gastric mucosa. The serum levels of IL-5 and such downstream molecules of STAT6 as CCL11/eotaxin-1, CCL24/eotaxin-2, and CCL26/eotaxin-3 were increased in both this patient and patients with EoG (Fig 3, *J*). IL-4 and IL-13 were rarely detected in the patient, whereas they were increased in the patients with EoG (Fig 3, *J*). Microarray analysis of the gastric mucosa showed this patient to have distinct gene expression profiles compared with the controls and patients with EoG, including upregulated gene expression of STAT6-, fibrosis-, and germinal center formation–related molecules (Fig 3, *K*).

Finally, to confirm the effects of p.Asp419Asn STAT6 protein *in vivo*, we generated knock-in mice having the corresponding mutation by using the CRISPER/Cas9 system. We found that 42.9% of homozygous mice and 3.3% of heterozygous mice spontaneously developed dermatitis with skin thickening and eosinophil infiltration (Fig 4, *A*, *B*, *C*, and *D*). Interestingly, the serum IgE levels, mRNA expressions of type-2 cytokines/chemokines in skin, and type-2 cytokine production from cervical lymph node cells were increased in both homozygous and heterozygous mice compared with WT mice, with or without development of spontaneous dermatitis (Fig 4, *E*, *F*, and *G*). We also induced atopic dermatitis–like skin inflammation by topical application of a vitamin D3 analog (MC903) in those mice[15] and found that MC903-treated heterozygous and homozygous mutant mice had greater skin thickening, inflammatory cell infiltration, and collagen fiber deposition in the dermal layer compared with MC903-treated WT mice (Fig 4, *H*, *I*, and *J*). These findings suggest that p.Asp419Asn STAT6 protein is involved in the development and exacerbation of atopic dermatitis–like skin inflammation accompanied by collagen fiber deposition in the dermal layer.

The clinical phenotypes of the patient—including early-onset multiple allergic diseases, a high serum IgE level, a high T_H2-cell proportion, and hypereosinophilia—might be explained by hyperactivation of STAT6 in its critical roles in T_H2-cell differentiation and in IgE class-switching in B cells.[1] Large polypoid nodules are not normally found in patients with EGID. Because STAT6 signaling is critically involved in germinal center formation[16,17] and its somatic mutation causes follicular lymphoma,[14] STAT6 hyperactivation might also be causing the nodule. Another unique finding in this patient, that is, the severe atopic dermatitis accompanied by increased dermal collagen fiber deposition, might also be explained by STAT6 hyperactivation because STAT6 activation reportedly upregulated TGF-β/Smad signaling and promoted fibrosis with extracellular matrix deposition and fibroblast proliferation.[18]

This report has several limitations to acknowledge. First, because this is a report of a single case, identifying additional patients with *STAT6* GOF variant would have been ideal. Second, it remains unclear how p.Asp419Asn STAT6 protein is translocated into the nucleus without undergoing phosphorylation and then enhances STAT6's transcriptional activity. Finally, although the effects of this *STAT6* variant varied depending on the organ and the patient's age, those mechanisms remain unclear. Further studies are needed to clarify these issues.

In conclusion, we have identified a novel *STAT6* GOF variant that is potentially involved in PADs with early-onset multiple allergic diseases, a high serum IgE level, hypereosinophilia, severe atopic dermatitis with increased dermal collagen fiber deposition, and EGIDs with numerous polypoid nodules in the pylorus and duodenal bulb. Regardless of the above-noted limitations, our report identifying this novel *STAT6* GOF variant will contribute to our understanding of PADs and might facilitate proper diagnosis of affected individuals, especially early-onset and severe cases carrying this and other *STAT6* variants, all over the world.

The detailed methods are presented in this article's Online Repository at www.jacionline.org.

We thank the patient and his family for their sincere efforts in cooperating with this study. We also thank the members of the National Research Institute for Child Health and Development (Ms Masako Fujiwara, Ms Chika Shirakawa, Ms Motomi Takami, Ms Emiko Matsuzaka, Mr Motohiro Kuriyama, Dr Saori Nagashima, Dr Rina Kusuda, Dr Tomoyuki Kawasaki, and Ms Miho Terao) for their invaluable assistance with the experiments. We also want to express our sincere gratitude to all the members of the National Center for Child Health and Development—especially the members of the Allergy Center, the Division of Gastroenterology, and the Department of Nutrition—for their assistance in treating the patient. We thank Mr Lawrence W. Stiver (Tokyo, Japan; Quality Translation Co., Ltd; qualityt@gol.com) for proofreading our manuscript. The graphical abstract was created with BioRender.com.

Clinical implications: A novel *STAT6* GOF variant contributed to multiple allergic diseases, high serum IgE, hypereosinophilia, severe atopic dermatitis with increased dermal collagen fiber deposition, and eosinophilic gastrointestinal disorder with polypoid nodules.

REFERENCES

1. Akdis M, Aab A, Altunbulakli C, Azkur K, Costa RA, Crameri R, et al. Interleukins (from IL-1 to IL-38), interferons, transforming growth factor beta, and TNF-alpha: receptors, functions, and roles in diseases. J Allergy Clin Immunol 2016;138:984-1010.
2. Schoettler N, Rodriguez E, Weidinger S, Ober C. Advances in asthma and allergic disease genetics: is bigger always better? J Allergy Clin Immunol 2019;144:1495-506.
3. Luo Y, Alexander M, Gadina M, O'Shea JJ, Meylan F, Schwartz DM. JAK-STAT signaling in human disease: from genetic syndromes to clinical inhibition. J Allergy Clin Immunol 2021;148:911-25.
4. Vaseghi-Shanjani M, Smith KL, Sara RJ, Modi BP, Branch A, Sharma M, et al. Inborn errors of immunity manifesting as atopic disorders. J Allergy Clin Immunol 2021;148:1130-9.
5. Seth N, Tuano KS, Chinen J. Inborn errors of immunity: recent progress. J Allergy Clin Immunol 2021;148:1442-50.
6. Okamoto K, Morio T. Inborn errors of immunity with eosinophilia. Allergol Int 2021;70:415-20.
7. Stadler PC, Renner ED, Milner J, Wollenberg A. Inborn error of immunity or atopic dermatitis: when to be concerned and how to investigate. J Allergy Clin Immunol Pract 2021;9:1501-7.
8. Lyons JJ, Milner JD. Primary atopic disorders. J Exp Med 2018;215:1009-22.
9. Wright BL, Schwartz JT, Ruffner MA, Furuta GT, Gonsalves N, Dellon ES, et al. Eosinophilic gastrointestinal diseases make a name for themselves: a new consensus statement with updated nomenclature. J Allergy Clin Immunol 2022;150:291-3.
10. Grimbacher B, Schaffer AA, Holland SM, Davis J, Gallin JI, Malech HL, et al. Genetic linkage of hyper-IgE syndrome to chromosome 4. Am J Hum Genet 1999;65:735-44.
11. Shahin T, Aschenbrenner D, Cagdas D, Bal SK, Conde CD, Garncarz W, et al. Selective loss of function variants in IL6ST cause hyper-IgE syndrome with distinct impairments of T-cell phenotype and function. Haematologica 2019;104:609-21.
12. Tanaka T, Yamashita A, Ichihara K. Reference intervals of clinical tests in children determined by a latent reference value extraction method. J Jpn Pediatr Soc 2008;112:1117-32.
13. Chen H, Sun H, You F, Sun W, Zhou X, Chen L, et al. Activation of STAT6 by STING is critical for antiviral innate immunity. Cell 2011;147:436-46.
14. Yildiz M, Li H, Bernard D, Amin NA, Ouillette P, Jones S, et al. Activating STAT6 mutations in follicular lymphoma. Blood 2015;125:668-79.
15. Matsumoto K, Morita H, Nakae S. New insights of human atopic dermatitis provided by mouse models. J Allergy Clin Immunol 2021;148:722-4.

16. Turqueti-Neves A, Otte M, Prazeres da Costa O, Hopken UE, Lipp M, Buch T, et al. B-cell-intrinsic STAT6 signaling controls germinal center formation. Eur J Immunol 2014;44:2130-8.
17. Sulczewski FB, Martino LA, da Silva Almeida B, Yamamoto MM, Rosa DS, Boscardin SB. STAT6 signaling pathway controls germinal center responses promoted after antigen targeting to conventional type 2 dendritic cells. Curr Res Immunol 2021;2:120-31.
18. Nguyen JK, Austin E, Huang A, Mamalis A, Jagdeo J. The IL-4/IL-13 axis in skin fibrosis and scarring: mechanistic concepts and therapeutic targets. Arch Dermatol Res 2020;312:81-92.

METHODS

DNA extraction

Genomic DNA of peripheral blood leukocytes was extracted using a Genomix kit (Biologica, Nagoya, Japan). Buccal mucosa was collected using an iSWAB DNA Collection Kit (Mawi DNA Technologies, Hayward, Calif), and the DNA was extracted using PrepIT-L2P reagent (DNA genoTek, Ottawa, Canada) in accordance with the manufacturer's instructions.

Whole-exome sequencing

Whole-exome sequencing analysis was performed for the patient and his parents using genomic DNA from peripheral blood. Next-generation sequencing libraries were enriched using the SureSelect Human All Exon V6 kit (Agilent Technology, Santa Clara, Calif) and sequenced using a HiSeq 2500 (Illumina, San Diego, Calif) with 100-bp paired-end reads. Sequence reads were aligned to GRCh38 using a Burrows–Wheeler aligner. Variants were called the GATK Unified Genotypes and annotated using ANNOVAR tools. High-quality variants were then narrowed down to those whose frequency was greater than 0.01 among gnomAD V3.1.2, 1000 genome, P8.3KJPN, and HGVD. We also used our in-house whole-exome variant database built with 3506 samples. The remaining variants related to protein coding including splicing were finally segregated under the assumption of being autosomal-dominant, autosomal-recessive, and X-linked dominant diseases. Other genetically cosegregated pathogenic variants were not found among genes associated with severe allergies. The segregated variants are summarized in Table E1 with their prediction scores of SIFT, Polyphen2, CADD. Using whole-exome sequencing data, copy number variants were detected by the read depth–based approach. In brief, read coverage in each target was converted to logarithmic ratios across the genome for each sample and normalized to a reference derived from 209 control samples. The calibrated $\log_2$ copy ratios were statistically validated. The detected copy number variants were classified according to the American College of Medical Genetics and Genomics guidelines.

Sanger sequencing of STAT6

Genomic DNA was amplified with a forward primer (5′-CAACCTGGGTGAGTCATGCAAGTCAC-3′) and a reverse primer (5′-GCTGGCACGTGTAAGCATTAGGATTG-3′) and directly sequenced with an inner reverse primer (5′-CTGCACCACTGCCCATGTTAGAAC-3′) using an AB I3130.

Deep sequencing

To confirm that the variant was of germline origin, deep sequencing of the variant in the blood and saliva was performed as follows. The first PCR was performed using the same primers as for the Sanger sequencing. PCR products were diluted to 100 pg/mL with water and used as the template for nested second PCR (forward primer, GTCTCTGCC CCTGGTGGTC ATCG; and reverse primer, AGAGCACTGCAGGCTACCGTCTTG). The nested PCR product was purified using a MinElute PCR Purification Kit (QIAGEN, Düsseldorf, Germany). Then, 250 ng of purified amplicons was subjected to library preparation using the GenNext NGS Library Kit (TOYOBO, Tokyo, Japan) and KAPA Dual-Indexed Adapter Kit for Illumina Platforms (KAPA BIOSYSTEMS, Wilmington, Mass) without postamplification. The prepared library was deep-sequenced using nano MiSeq Reagent Kits v2 (Illumina) for 300 cycles. It revealed an almost 1:1 ratio of reference to variant alleles in both tissues, as presented in Table E2.

STAT6 expression-plasmid cell transfection and luciferase reporter assays

STAT6 WT or STAT6 mutant expression vectors were constructed by inserting the synthesized *STAT6* or mutant *STAT6* (c.1255G> A) complementary DNA (cDNA) into a pcDNA3.1 vector. The synthesized cDNA of *STAT6* (NM_003153.5) or mutant *STAT6* carried by the pUC19 vector was purchased from FASMAC Co., Ltd (Kanagawa, Japan). The WT *STAT6* and mutant *STAT6* were digested and cloned into the EcoRI/XhoI site of the pcDNA3.1 expression vector. DNA fragments containing human eotaxin-3 were amplified from genomic DNA using a forward primer (5′-AATCTCGAGTTTTATTTCTAGTGGGGA-3′) and a reverse primer (5′-ATTAAGCTTGTAGATGCT GCAAATCAGGC-3′). The PCR fragments were digested with XhoI and HindIII and cloned into pGL-4.2. An eotaxin-3 promoter-reporter plasmid with a point mutation in the *STAT6*-binding site was generated using the PrimeSTAR Mutagenesis Basal Kit (Takara Bio, Inc, Shiga, Japan) according to the manufacturer's protocol. 5′-AGCTCTGGAATTGTTTTCAGGGCCGTCT-3′ and 5′-TTCCAGAGCTTTCTGTGGTTGGGAACAG-3′ primers were used for the *STAT6*- binding-site mutation. All plasmids were analyzed by Sanger sequencing for sequence confirmation. Luciferase reporter assays were performed according to a previously published method,[E1] with minor modifications. HEK293 cells were seeded into 96-well plates at 1×10^4 cells/well. At 24 hours after seeding, the cells were transiently transfected with 0.1 μg of eotaxin-3 promoter-reporter plasmid, together with 0.9 μg of plasmids encoding either wild or mutant STAT6, and 0.01 μg of *Renilla* luciferase plasmid using Lipofectamine 3000 (Thermo Fisher Scientific, Waltham, Mass). Twenty-four hours later, the cells were cultured with or without 10 ng/mL of human recombinant IL-4 (PeproTech, Cranbury, NJ) and then cultured for an additional 24 hours. The luciferase activities were then measured using a Dual-Glo Luciferase Assay System (Promega, Madison, Wis). Representative data of 2 independent experiments are shown in Fig 2.

Flow cytometric analysis of human PBMCs

Human PBMCs were isolated from heparinized blood from patients and healthy adult volunteers by density-gradient centrifugation using pluriSelect (pluriSelect Life Science UG & Co. KG, Leipzig, Germany). Cell surface proteins were stained using the following antibodies: fluorescein isothiocyanate-conjugated anti-CD3; PerCP/Cy5.5–conjugated anti-CD4; Alexa 700–conjugated anti-CD45RA; Brilliant Violet 510–conjugated anti-CD45 (all from BioLegend, San Diego, Calif); and Alexa 647–conjugated anti–chemoattractant receptor expressed on T_H2 cells (BD Biosciences, Franklin Lakes, NJ). Subsequently, the cells were fixed, permeabilized, and stained with phycoerythrin (PE)-conjugated anti-STAT6 phospho antibody or PE-conjugated mouse IgG1κ isotype antibody using FOXP3 Fix/Perm Buffer Set (all from BioLegend). The cells were analyzed using an LSR Fortessa (BD Bioscience). T_H2 cells were defined as $CD45^+CD3^+CD4^+$chemoattractant receptor expressed on T_H2^+ cells.

Establishment of human LCLs

Human LCLs were established by SRL, Inc (Tokyo, Japan). In brief, mononuclear cells isolated from 2 mL of peripheral blood using Lymphoprep (Nacalai Tesque, Kyoto, Japan) were immortalized for 30 minutes in culture medium of B95-8 EBV-producing marmoset cell line. The culture medium was then replaced with 1 mL of RPMI1640 containing 20% of HyClone FBS, 5 μg/mL Cyclosporin A (Cat# C-3662, Merck, Darmstadt, Germany), and 100 unit/mL penicillin-streptomycin (Cat# 1514012, ThermoFisher, Waltham, Mass). The cells were incubated while changing half of the culture medium to fresh medium every day. After 10 days, the medium was completely replaced with prewarmed, freshly prepared medium, that is, RPMI1640 containing 20% of HyClone FBS.

Protein isolation and Western blotting of LCLs

LCLs derived from patients or parents were treated with 10 ng/mL IL-4 for 0.5, 3, and 6 hours, respectively, and the respective cells and untreated cells (shown as 0h) were harvested. For protein samples from whole-cell lysates, cells were lysed on ice in RIPA buffer (#16488-34; Nacalai tesque, Inc, Kyoto, Japan) supplemented with complete protease inhibitor cocktail (Sigma-Aldrich, St Louis, Mo), and then the protein concentration was measured. For the protein samples of cytoplasmic and nucleic fractions, fractionation and protein extraction were performed using NE-PER Nuclear and Cytoplasmic Extraction Reagents (#78833; Pierce Biotechnology, Rockford, Ill). The samples were separated on SDS-PAGE gel and then transferred to

polyvinylidene difluoride (PDVF) membranes. Western blotting was performed using primary antibodies, anti-STAT6 rabbit mAb (#9362; Cell Signaling Technology, Danvers, Mass), anti–Phospho-Stat6 (Tyr641) antibody (#9361; Cell Signaling Technology), anti-glyceraldehyde-3-phosphate dehydrogenase (GAPDH) (14C10) rabbit mAb (#2118; Cell Signaling Technology), anti-HSP90 (E289) antibody (#4875; Cell Signaling Technology), and anti-HDAC2 antibody (#2540; Cell Signaling Technology). Horseradish peroxidase–conjugated goat antirabbit IgG antibody (#7074; Cell Signaling Technology) was used as the secondary antibody.

Flow cytometric analysis of LCLs

Phosphorylation kinetics. LCLs were cultured with 10 ng/mL of human recombinant IL-4 for 15, 30, and 60 minutes. The cells were fixed, permeabilized, and stained with PE-conjugated anti-STAT6 phospho antibody (#686004; BioLegend) or PE-conjugated mouse IgG1κ isotype antibody (#400114; BioLegend) using FOXP3 Fix/Perm Buffer Set (all from BioLegend). The cells were analyzed using FACSymphony (BD Bioscience).

Effects of JAK inhibitors. LCLs were pretreated with ruxolitinib (0.5 or 5 μM; Chemscene, Monmouth Junction, NJ) or tofacitinib (0.5 or 5 μM; Selleckchem, Houston, Tex) for 2 hours and stimulated with human recombinant IL-4 (10 ng/mL) for 1 hour. Their STAT6 phosphorylation was determined as described above.

Serum cytokine analysis

Sera were prepared from the patient with STAT6 variant, patients with IgE-mediated food allergy (n = 4), and patients with EoG (n = 3) and stored at −80°C until use. The patients with EoG had been diagnosed on the basis of histological findings of significant eosinophil infiltration. The levels of cytokines and chemokines were determined using a Luminex multiplex cytokine analysis kit (Merck) according to the manufacturer's instructions.

Transcriptome analysis of the gastric mucosa

Biopsy specimens of the gastric mucosa were collected from the patients and the controls and stored at −80°C until use. The patients with EoG had been diagnosed on the basis of histological findings of significant eosinophil infiltration. The controls were individuals who were suspected of having gastrointestinal disorders but showed no histological abnormalities. Total RNA was extracted from preserved biopsy samples using an RNeasy Mini Kit (Qiagen, Valencia, Calif). Gene expression analysis was performed using Agilent SurePrint G3 Human GE 8 x 60k microarrays (Agilent Technologies, Santa Clara, Calif) according to the manufacturer's instructions. Data were normalized and analyzed using Subio Platform software (Subio, Kagoshima, Japan).

Generation of *Stat6* mutant mice

The guide RNA (gRNA) against *Stat6* used in this study was 5′-TAGCTTTGGCGTTGTTGTcTTGG-3′, in which the target of nucleotide substitution is designated by a lowercase letter; it was designed using CRISPRdirect.[E2] Single gRNA was synthesized using *Stat6*_gRNA1 temp 5′-CTAATACGACTCACTATAGTAGCTTTGGCGTTGTTGTcTGTTTTAGAGCTAGAAATAGCA-3′ and a CUGA7 gRNA Synthesis Kit (Nippon Gene, Toyama, Japan) according to the manufacturer's instructions. The single-stranded oligodeoxynucleotide (ssODN) used in this study was Stat6_sub_s-sODN 5′- CTGTCTCTGCCCTTGGTGGTCATCGTGCATGGTAACCAAaACAACAACGCCAAAGCTACCATCCTATGGGACAATGCCT-3′. C57BL/6J mice were purchased from SLC Japan (Shizuoka, Japan), and embryos were collected after *in vitro* fertilization. A mixture of 250 ng/μL single gRNA, 100 ng/μL ssODN, and 100 ng/μL Cas9 protein (Nippon Gene) was injected into the pronuclei and cytoplasm of the zygotes. After overnight culture, embryos that reached the 2-cell stage were transferred into the oviduct of pseudopregnant ICR female mice (SLC Japan). The primers used in PCR analysis of the genotypes were Stat6genoF1 5′-CCAGTGATGCACTACCAACC-3′ and Stat6genoR2 5′-GGACAGCCCGTTATCTCACC-3′. The genotypes of the knock-in mice were confirmed by Sanger sequencing, as shown in Fig E1. All animal protocols were approved by the Animal Care and Use Committee of the National Research Institute for Child Health and Development, Tokyo, Japan.

Vitamin D3 analog-induced atopic dermatitis model

C57BL/6J WT mice, *Stat6*$^{D419N/wt}$ heterozygous mice, and *Stat6*$^{D419N/D419N}$ homozygous mice were topically treated on unilateral ears with 1 nmol of MC903 (calcipotriol; Tocris Bioscience, Bristol, United Kingdom) in 20 μL of ethanol or vehicle alone, every other day for a total of 7 times. The ear thickness was measured before topical applications. One day after the last topical application, the mice were euthanized for examination.

Quantitative real-time PCR

Mouse ears were harvested and stored in RNAlater (Thermo Fisher Scientific). The tissues were immersed in QIAzol (QIAGEN) and homogenized using BioMasher (Kanto Kagaku, Tokyo, Japan). Total RNA was isolated using a ReliaPrep RNA Tissue Miniprep System (Promega) according to the manufacturer's instructions. RNA concentrations were measured with Nanodrop 2000c (Thermo Fisher Scientific), and cDNA was synthesized using an iScript cDNA Synthesis kit (Bio-Rad, Hercules, Calif). Quantitative real-time PCR was performed on a CFX96 Touch Deep Well Real-Time PCR System (Bio-Rad) with the TaqMan gene expression systems (Thermo Fisher Scientific) listed below: *Gapdh* (Mm99999915_g1), *Il4* (Mm00445259_m1), *Il5* (Mm00439646_m1), *Il13* (Mm00434204_m1), *Ccl11*/*Eotaxin 1* (Mm00441238_m1), and *Ccl24*/*Eotaxin 2* (Mm00444701_m1). Delta threshold cycle (ΔCt) values of each sample were determined using *Gapdh* as a reference gene, and $2^{-\Delta\Delta Ct}$ was calculated with the average gene expression of WT mice as a reference.

Preparation of epidermal and dermal cells from mice

The ears were split into dorsal and ventral halves and incubated with 0.25% trypsin/EDTA solution (Sigma-Aldrich) for 45 minutes at 37°C. Then, epidermal sheets were separated from the dermal sheets with a forceps. For isolation of epidermal cells, the epidermal sheets were dissociated in HBSS solution using gentleMACS Dissociator (Miltenyi Biotec, Bergisch Gladbach, Germany). For isolation of dermal cells, the dermal sheets were minced and incubated in PBS supplemented with 1% BSA, 400 units/mL collagenase type 2 (Worthington, Lakewood, NJ), 1000 units/mL hyaluronidase type 4-S (Sigma-Aldrich), and 50 units/mL DNase 1 (Roche, Basel, Switzerland) for 60 minutes at 37°C, followed by dissociation using a gentleMACS Dissociator. After the dissociated sheets were passed through a nylon filter (70 μm; Corning, Corning, NY), epidermal and dermal cell suspensions were collected.

Flow cytometric analysis of epidermal and dermal cells

Single-cell suspensions of ears were incubated with antimouse CD16/CD32 mAb (2.4G2; BD Bioscience) in HANKS Buffer containing 2% FCS for FcR blocking. Cell surface molecules were stained with the following antibodies: APC-R700–conjugated anti–sialic acid-binding immunoglobulin-like lectin (Siglec)-f and BUV395-conjugated anti-CD45 (BD Bioscience). After staining, the cells were analyzed using Symphony (BD Bioscience). Eosinophils were defined as $CD45^{+}Siglec\text{-}F^{+}$cells.

Culture of cervical lymph node cells

Cervical lymph nodes were collected, and cells were isolated using a 70-μm cell strainer (Corning, Glendale, Ala). The cells were cultured with 20 ng/mL of phorbol 12-myristate 13-acetate (Sigma-Aldrich) and 500 ng/mL of ionomycin (Fujifilm Wako, Osaka, Japan) for 72 hours. The levels of IL-4 and

IL-13 in the culture supernatants were determined by ELISA (Thermo Fisher Scientific). All procedures were performed in accordance with the manufacturers's instructions.

Measurement of immunoglobulin in sera

The total IgE in sera was quantified by ELISA, as described elsewhere.[E3] Biotinylated antimouse IgE (R35-118) and horseradish peroxidase–conjugated streptavidin were obtained from BD Biosciences and used as detection antibodies/reagents.

Histology

The ears were fixed in 4% paraformaldehyde phosphate buffer solution (Fujifilm Wako), embedded in paraffin, and sliced into 5-μm–thick sections. The histology was examined by hematoxylin-eosin staining and Masson's trichrome staining. Collagen fibers were quantified by ImageJ software (http://imagej.nih.gov/ij/).

Statistical analysis

Data were analyzed using GraphPad Prism v9.1.2 (GraphPad Software, Inc, San Diego, Calif). Two-group data sets were analyzed using the Mann-Whitney *U* test, and 3-group data sets were analyzed using the Kruskal-Wallis test. A *P* value of less than or equal to .05 was considered statistically significant.

REFERENCES

E1. Luo Y, Alexander M, Gadina M, O'Shea JJ, Meylan F, Schwartz DM. JAK-STAT signaling in human disease: from genetic syndromes to clinical inhibition. J Allergy Clin Immunol 2021;148:911-25.

E2. Naito Y, Hino K, Bono H, Ui-Tei K. CRISPRdirect: software for designing CRISPR/Cas guide RNA with reduced off-target sites. Bioinformatics 2015;31:1120-3.

E3. Suzukawa M, Morita H, Nambu A, Arae K, Shimura E, Shibui A, et al. Epithelial cell-derived IL-25, but not Th17 cell-derived IL-17 of IL-17F, is crucial for murine asthma. J Immunol 2012;189:3641-52.

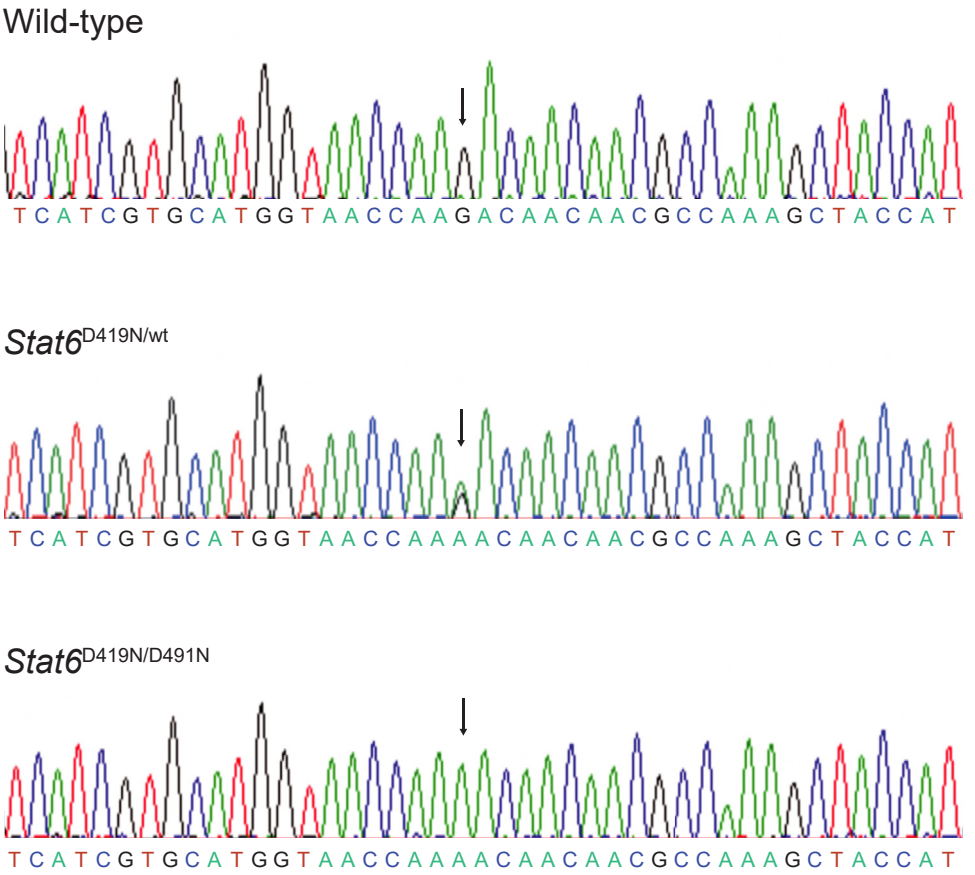

FIG E1. Representative electropherograms of WT, Stat6$^{D419N/wt}$, and Stat6$^{D419N/D419N}$. Target nucleotides are indicated with red circles.

TABLE E1. Segregated rare variants in the trio-based whole-exome sequence analysis

Chr	Position (GRCh38)	Gene	RefSeq_ID	Nucleotide	Amino acid	dbSNP155	ClinVar	SIFT	Poly Phen-2	CADD_ phred	gnomAD	1000G_all	8.3K JPN	HGVD	In-house	Proband	OMIM
1	201212038	*IGFN1*	NM_001164586.2	c.7145G>A	p.G2382D	rs1172017208	NA	Tolerated	NA	13.3	NA	NA	NA	NA	NA	*de novo*	NA
12	57102879	*STAT6*	NM_003153.5	c.1255G>A	p.D419N	rs11172102	NA	Damaging	Probably damaging	31.0	NA	NA	NA	NA	NA	*de novo*	NA
X	74521057	*SLC16A2*	NM_006517.5	c.498C>G	p.D166E	NA	NA	Tolerated	Benign	22.9	NA	NA	NA	NA	NA	Inherited from mother	Allan-Herndon-Dudley syndrome [300523]
X	106206201	*MUM1L1*	NM_152423.5	c.769G>A	p.E257K	rs755979209	NA	Tolerated	Possibly damaging	23.0	3.58×10^{-05}	0.0005298	0.0001	NA	NA	Inherited from mother	NA

dbSNP155 (https://www.ncbi.nlm.nih.gov/snp/); ClinVar (https://www.ncbi.nlm.nih.gov/clinvar/); SIFT (https://sift.bii.a-star.edu.sg/); PolyPhen-2 (http://genetics.bwh.harvard.edu/pph2/); CADD (https://cadd.gs.washington.edu/); gnomAD (https://gnomad.broadinstitute.org/); 1000G_all (https://www.internationalgenome.org/); 8.3KJPN (https://jmorp.megabank.tohoku.ac.jp/202102/variants/); HGVD (https://www.hgvd.genome.med.kyoto-u.ac.jp/).
NA, Not available.

TABLE E2. Deep sequencing data of the STAT6 variant in the patient

Tissue	Total count	Count of Ref: C	Count of Alt: T	Allele frequency of Ref	Allele frequency of Alt
Blood	7481	3808	3649	0.51	0.49
Saliva	7200	3725	3452	0.52	0.48

Alt, Alternative allele; *Ref*, reference allele.